ROUTING AND ACTION

MEMORANDUM

ROUTING

TO: (1) Materials Science Division (Prater, John)

Report is available for review

(2) Proposal Files Proposal No.: 56987MS.1

DESCRIPTION OF MATERIAL

CONTRACT OR GRANT NUMBER: W911NF-10-1-0362

INSTITUTION: University of Wisconsin - Madison

PRINCIPAL INVESTIGATOR: Chang-Beom Eom

TYPE REPORT: New Reprint

DATE RECEIVED: 9/8/2011 7:31:09PM

PERIOD COVERED: through

TITLE: Structural Consequences of Ferroelectric Nanolithography

ACTION TAKEN BY DIVISION

(x) Report has been reviewed for technical sufficiency and IS [x] IS NOT [ ] satisfactory.

(x) Material has been given an OPSEC review and it has been determined to be non sensitive and, except for manuscripts and progress reports, suitable for public release.

Approved by SSL\JOHN.PRATER on 2/13/2012 3:44:22PM

ARO FORM 36-E

REPORT DOCUMENTATION PAGE

Form Approved OMB NO. 0704-0188

1. REPORT DATE (DD-MM-YYYY)	2. REPORT TYPE	3. DATES COVERED (From - To)
	New Reprint	-

4. TITLE AND SUBTITLE
Structural Consequences of Ferroelectric Nanolithography

5a. CONTRACT NUMBER
W911NF-10-1-0362

5b. GRANT NUMBER

5c. PROGRAM ELEMENT NUMBER
611102

6. AUTHORS
Ji Young Jo, Pice Chen, Rebecca J. Sichel, Seung-Hyub Baek, Ryan T. Smith, Nina Balke, Sergei V. Kalinin, Martin V. Holt, Jo?rg Maser, Kenneth Evans-Lutterodt, Chang-Beom Eom, Paul G. Evans

5d. PROJECT NUMBER

5e. TASK NUMBER

5f. WORK UNIT NUMBER

7. PERFORMING ORGANIZATION NAMES AND ADDRESSES
University of Wisconsin - Madison
The Board of Regents of the University of Wisconsin System
Suite 6401
Madison, WI 53715 -1218

8. PERFORMING ORGANIZATION REPORT NUMBER

9. SPONSORING/MONITORING AGENCY NAME(S) AND ADDRESS(ES)
U.S. Army Research Office
P.O. Box 12211
Research Triangle Park, NC 27709-2211

10. SPONSOR/MONITOR'S ACRONYM(S)
ARO

11. SPONSOR/MONITOR'S REPORT NUMBER(S)
56987-MS.1

12. DISTRIBUTION AVAILIBILITY STATEMENT
Approved for public release; distribution is unlimited.

13. SUPPLEMENTARY NOTES
The views, opinions and/or findings contained in this report are those of the author(s) and should not contrued as an official Department of the Army position, policy or decision, unless so designated by other documentation.

14. ABSTRACT
Domains of remnant polarization can be written into ferroelectrics with nanoscale precision using scanning probe nanolithography techniques such as piezoresponse force microscopy (PFM). Understanding the structural effects accompanying this process has been challenging due to the lack of appropriate structural characterization tools. Synchrotron X-ray nanodiffraction provides images of the domain structure written by PFM into an epitaxial Pb(Zr,Ti)O3 thin film and simultaneously

15. SUBJECT TERMS
Ferroelectrics, X-ray nanodiffraction, domain nanolithography, strain, coherent X-ray diffraction

16. SECURITY CLASSIFICATION OF:			17. LIMITATION OF ABSTRACT	15. NUMBER OF PAGES	19a. NAME OF RESPONSIBLE PERSON
a. REPORT	b. ABSTRACT	c. THIS PAGE			Chang-Beom Eom
UU	UU	UU	UU		19b. TELEPHONE NUMBER: 608-263-6305

Report Title

Structural Consequences of Ferroelectric Nanolithography

ABSTRACT

Domains of remnant polarization can be written into ferroelectrics with nanoscale precision using scanning probe nanolithography techniques such as piezoresponse force microscopy
(PFM). Understanding the structural effects accompanying this process has been challenging due to the lack of appropriate structural characterization tools. Synchrotron X-ray nanodiffraction
provides images of the domain structure written by PFM into an epitaxial Pb(Zr,Ti)O3 thin film and simultaneously reveals structural effects arising from the writing process. A coherent scattering
simulation including the superposition of the beams simultaneously diffracted by multiple mosaic blocks provides an excellent fit to the observed diffraction patterns. Domains inwhich the polarization is reversed from the as-grown state have a strain of up to 0.1% representing the piezoelectric response to unscreened surface charges. An additional X-ray microdiffraction study of the photon-energy dependence of the difference in diffracted intensity between opposite polarization states shows that this contrast has a crystallographic origin.The sign and magnitude of the intensity contrast between domains of opposite polarization are consistent with the polarization expected from PFM images and with the writing of domains through the entire thickness of the ferroelectric layer. The strain induced by writing provides a significant additional contribution to the increased free energy of the written domain state with respect to a uniformly polarized state.

REPORT DOCUMENTATION PAGE (SF298)
(Continuation Sheet)

Continuation for Block 13

ARO Report Number 56987.1-MS
Structural Consequences of Ferroelectric Nanoli ...

Block 13: Supplementary Note

Approved for public release; distribution is unlimited.

NANO LETTERS

LETTER

pubs.acs.org/NanoLett

Structural Consequences of Ferroelectric Nanolithography

Ji Young Jo,[†,⊥] Pice Chen,[†] Rebecca J. Sichel,[†] Seung-Hyub Baek,[†] Ryan T. Smith,[†] Nina Balke,[‡] Sergei V. Kalinin,[‡] Martin V. Holt,[§] Jörg Maser,[§] Kenneth Evans-Lutterodt,[∥] Chang-Beom Eom,[†] and Paul G. Evans*[,†]

[†]Department of Materials Science and Engineering and Materials Science Program, University of Wisconsin, Madison, Wisconsin 53706, United States

[‡]Center for Nanophase Materials Sciences, Oak Ridge National Laboratory, Oak Ridge, Tennessee 37831, United States

[§]Center for Nanoscale Materials, Argonne National Laboratory, Argonne, Illinois 60439, United States

[∥]National Synchrotron Light Source, Brookhaven National Laboratory, Upton, New York 11973, United States

Supporting Information

ABSTRACT: Domains of remnant polarization can be written into ferroelectrics with nanoscale precision using scanning probe nanolithography techniques such as piezoresponse force microscopy (PFM). Understanding the structural effects accompanying this process has been challenging due to the lack of appropriate structural characterization tools. Synchrotron X-ray nanodiffraction provides images of the domain structure written by PFM into an epitaxial $Pb(Zr,Ti)O_3$ thin film and simultaneously reveals structural effects arising from the writing process. A coherent scattering simulation including the superposition of the beams simultaneously diffracted by multiple mosaic blocks provides an excellent fit to the observed diffraction patterns. Domains in which the polarization is reversed from the as-grown state have a strain of up to 0.1% representing the piezoelectric response to unscreened surface charges. An additional X-ray microdiffraction study of the photon-energy dependence of the difference in diffracted intensity between opposite polarization states shows that this contrast has a crystallographic origin. The sign and magnitude of the intensity contrast between domains of opposite polarization are consistent with the polarization expected from PFM images and with the writing of domains through the entire thickness of the ferroelectric layer. The strain induced by writing provides a significant additional contribution to the increased free energy of the written domain state with respect to a uniformly polarized state.

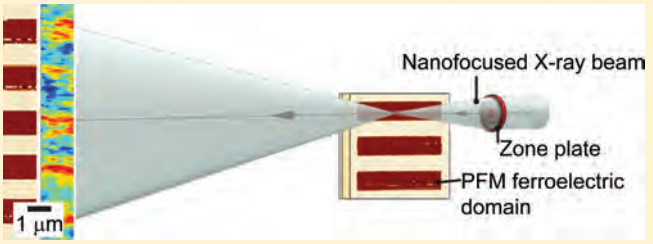

KEYWORDS: Ferroelectrics, X-ray nanodiffraction, domain nanolithography, strain, coherent X-ray diffraction

Developing the means to manipulate nanoscale patterns and thermodynamic order parameters at their fundamental length scales has been a persistent challenge in nanotechnology. Breakthroughs in scanning probe lithography have led to revolutionary control over the size and location of nanostructures,[1] the arrangement of functional chemical groups,[2,3] ferroelectric and magnetic domains,[4,5] and ferroelectric structural phases.[6] Ferroelectric nanotechnologies, such as memories, have not taken full advantage of these capabilities, in part because the physics of the lithographic processes and the effects of structural changes induced in the sample during lithography have not yet been sufficiently described. Here we probe the subtle structural distortion accompanying scanning-probe ferroelectric nanolithography, a widely used means of producing arbitrary nanoscale polarization domain patterns. Using X-ray nanodiffraction, a structural tool matched to the length scale of the written domains, we find that a domain pattern written into a ferroelectric $Pb(Zr,Ti)O_3$ (PZT) thin film is accompanied by a compressive strain of up to 0.1% in the written domains. This strain represents the electromechanical response to unscreened charges at surfaces and interfaces. The resulting increase in the free energy of domains introduced by the writing process poses an important limit for ferroelectric nanolithography.

Piezoresponse force microscopy (PFM) provides the means to manipulate and probe ferroelectric polarity with domain sizes down to the order of 1−10 nm (Figure 1a)[4] but provides relatively little information about the atomic-scale structure written into the ferroelectric layer along with the ferroelectric polarization. The structural interpretation of scanning probe data is challenging due to the complex interaction between the tip and the surface of the ferroelectric[7] and because scanning probes are most sensitive to near-surface layers. Structural effects are, however, crucially important in ferroelectrics and related materials because the lattice distortion is directly connected to the ferroelectric polarization via electromechanical coupling. Here we complement PFM with X-ray nanodiffraction in order to image the written domains and to obtain direct local structural information without the complexity arising from probe−surface interactions. It has been a challenge in the past to match the 10 to 100 nm scale of the features in the nanolithographic realm to the conventionally large size of X-ray beams. Synchrotron nanobeam

Received: March 24, 2011
Revised: May 30, 2011

dx.doi.org/10.1021/nl2009873 | *Nano Lett.* XXXX, XXX, 000–000

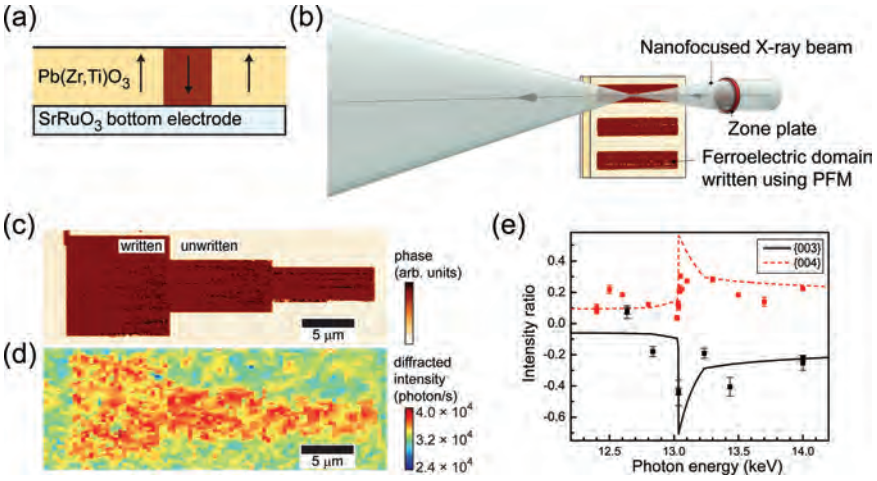

Figure 1. (a) A reversed polarization domain in a ferroelectric thin film. (b) X-ray domain imaging based on a scanning 50 nm diameter probe beam. (c) PFM image and (d) map of diffracted X-ray intensity using {002} reflections of a domain pattern consisting of three rectangles written using PFM. (e) Measured (symbols) and predicted (lines) photon-energy dependence of the intensity contrast between P_+ and P_- domains for the {003} and {004} reflections of PZT.

diffraction methods allow individual domains to be probed, providing local diffraction patterns that can be quantitatively interpreted to determine the distortion of the lattice.

A series of ferroelectric polarization domain patterns were nanolithographically written into an epitaxial ferroelectric $PbZr_{0.45}Ti_{0.55}O_3$ (PZT) film. PZT films were deposited using off-axis radio frequency sputtering onto $SrRuO_3/SrTiO_3$ substrates in which the $SrRuO_3$ layer served as a continuous bottom electrode. Imaging and poling in PFM experiments were performed using 160 nm thick PZT layers without top electrodes. Domains were written and read via PFM using a Pt/Ir coated tip. The tip voltage was +8 V during domain writing. During imaging, the tip was biased with an ac voltage of 0.5 V at approximately 300 kHz, close to the contact resonance frequency to increase the signal-to-noise ratio. The PFM phase and amplitude were separately recorded and analyzed.

Nanodiffraction studies of samples with written domains were performed using the X-ray nanoprobe at Sector 26 of the Advanced Photon Source, shown schematically in Figure 1b. The incident X-ray beam from an undulator insertion device was focused to a 50 nm full width at half-maximum spot by a Fresnel zone plate. The photon energy was varied during the experiment from 11.6 and 11.8 keV using a Si(111) monochromator. Differential scanning of the X-ray focusing optic relative to the sample was performed with a step size as small as 2−4 nm and a stability of ~10 nm over periods of hours to days using a hybrid optomechanical scanning nanopositioner.[8] Real-space X-ray nanobeam maps were acquired by rastering the sample and measuring the diffracted intensity using a photon-counting scintillation detector. Photon-energy scans allowed diffraction information to be collected without rotating the sample. The diffraction patterns were recorded with a direct-illumination charge-coupled device located 700 mm from the sample in a horizontal diffraction geometry.

The ferroelectric polarization was locally switched from the as-grown state in which the polarization is parallel to the surface normal (upward, bright in our PFM phase images in Figure 1c) to downward (dark in the PFM phase images). In the absence of boundary conditions making one polarization energetically favorable, the two polarization states nominally have the same free energy per unit volume and the free energy is minimized when the system selects a domain pattern with an area fraction $\alpha = 1/2$ of the sample in the upward polarization. The initial formation of the bottom-electrode/ferroelectric interface during the epitaxial growth of the PZT layers, however, lowers the free energy of the upward polarization state and moves the minimum energy to the uniformly poled $\alpha = 1$ state.[9] Nanolithographically written domains perturb the film from this low-energy configuration, and the lithographically written state is thus metastable.[10] We show here that writing domains also results in an elastic contribution to the total energy, further raising the free energy difference between the written state and the low-energy $\alpha = 1$ state. The as-grown state in effect serves as the control sample for our study of structural effects arising from the writing process.

The large numerical aperture Fresnel zone plate optic required to focus X-rays to a 50 nm spot produces a convergent partially coherent X-ray beam, which must be taken into account when analyzing nanodiffraction patterns.[11] The intensity of diffraction from the PZT layer depends on the polar orientation of the noncentrosymmetric PZT unit cell, and intensity maps acquired using scanning X-ray diffraction thus provide an easily interpreted map of ferroelectric domains.[12] The polarization-related intensity contrast arises because domains with opposite polarization produce X-ray reflections at the same angles but with crystallographic indices of opposite sign, e.g., 002 and $00\bar{2}$. The corresponding polarization states, which we label P_+ and P_-, are produced by applying a positive or negative voltage at the surface, respectively. In these states, the positively charged central Zr and Ti atoms are displaced down (P_+) or up (P_-), from the center of the tetragonal unit cell. The domain pattern written by PFM in Figure 1c is apparent in scanning nanodiffraction images of these {002} reflections shown in Figure 1d.

A quantitative basis for the interpretation of the nanobeam diffraction intensity is provided by measuring the polarization contrast of the {003} and {004} pairs of reflections at photon energies near the Pb L_3 absorption edge using 80 nm thick PZT layers with Pt top electrodes. These experiments were conducted at station X-13B of the National Synchrotron Light Source. The stored polarization was switched throughout an entire capacitor using voltages applied to the top electrode. The intensity contrast between polarization states (Figure 1e), defined as

dx.doi.org/10.1021/nl2009873 |*Nano Lett.* XXXX, XXX, 000–000

$(I(P_+) - I(P_-))/(I(P_+))$, agrees with a kinematic X-ray diffraction prediction using bulk atomic positions, a random-alloy distribution of Zr and Ti, and tabulated atomic scattering factors.[13−15] The sign of the contrast between polarization states, in particular, is different between families of reflections $\{00l\}$ in which l is odd (as $\{003\}$) and reflections with even l (e.g., $\{004\}$). The sign of the intensity contrast between domains in Figure 1d shows directly and crystallographically that nanolithography with a positive tip voltage has written domains with the expected polarity.

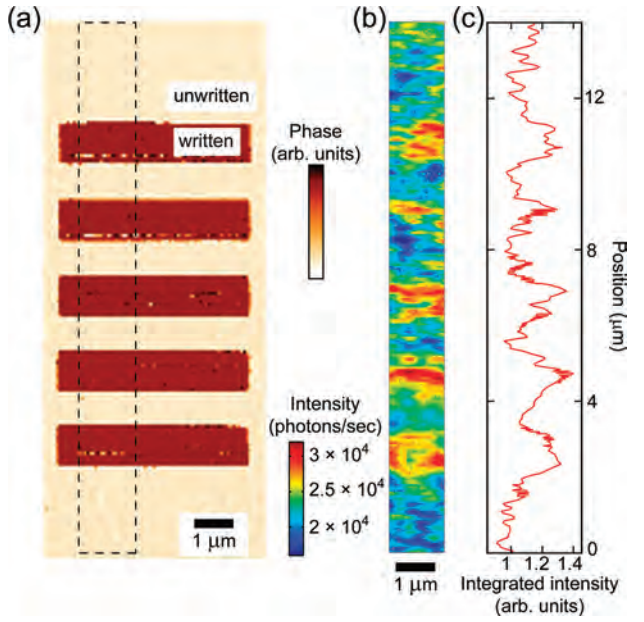

Figure 2. (a) PFM image of domains written by PFM. (b) Map of diffracted X-ray intensity in the dashed rectangle in (a). (c) Intensity as a function of vertical position, integrating over the horizontal direction of (b).

The PZT films have a complex microstructure in which crystallographic mosaic blocks are distributed over a range of orientations such that several blocks fall within the spatial and angular extent of the X-ray nanobeam. The sensitivity of the X-ray nanodiffraction to the existence of the mosaic blocks produces large variations in the diffracted intensity, illustrating the superposition of microstructural and polarization information in these images. The total change in diffracted intensity at domain walls occurs over a wider region in X-ray nanodiffraction images (Figure 1d) than in PFM images (Figure 1c). The distinction between effects arising from the mosaicity of the PZT layer and the intensity contrast arising from domains can be better seen in the comparison of PFM and nanodiffraction images of a set of 1 μm wide domains (Figure 2a,b). The integrated intensity along each stripe, shown in Figure 2c, clearly reveals the nanolithographic domains.

X-ray nanobeam diffraction provides atomic-scale structural information from which the structural consequences of the domain writing process can be determined. The diffraction patterns of the PZT layers are a coherent superposition of diffraction from several crystallographic mosaic blocks excited by the large 0.25° convergence of the focused beam, an effect which we include in a detailed analysis (see Supporting Information). Panels a and b of Figure 3 show X-ray diffraction patterns acquired from areas separated by 200 nm on opposite sides of a domain wall, within unwritten and written domains, respectively. These two regions fortuitously shared the same

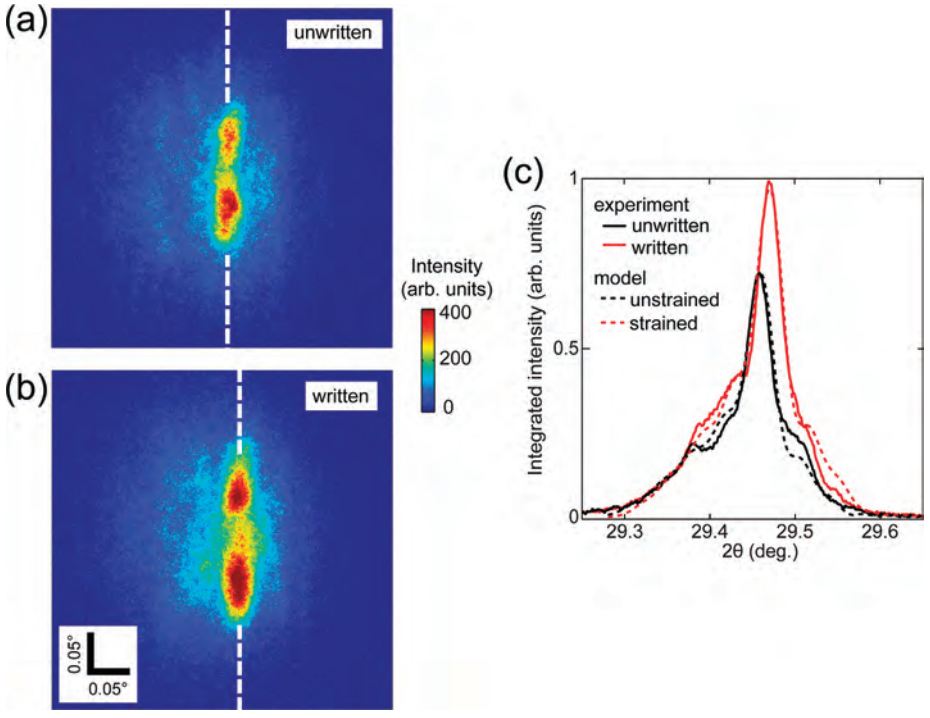

Figure 3. X-ray nanodiffraction patterns acquired with a photon energy of 11.75 keV from (a) unwritten and (b) written domains within the region of the images in panels a and b of Figure 2. The decrease in the intensity near the vertical center of the strong diffraction feature is an artifact due to the intensity profile imprinted on the incident beam by the central stop X-ray optical element. The 2θ angle of the maximum intensity, indicated by the dashed lines, is higher in the domains written by PFM. (c) Comparison of the diffracted intensity integrated over the vertical diffraction angle (solid lines) and coherent X-ray diffraction simulations (dashed lines).

dx.doi.org/10.1021/nl2009873 |*Nano Lett.* XXXX, XXX, 000–000

mosaic block structure. The diffraction patterns from the written and unwritten areas differ at large values of 2θ, the angle between the directions of the average incident beam and the observed diffracted beam. The difference can be seen in the diffraction patterns in panels a and b of Figure 3 as well as in the integrated 2θ dependence of the intensity in Figure 3c. The coherent diffraction analysis shows that the difference in intensity at high 2θ angles arises from a compressive strain in written areas.

The 2θ angles associated with the central peaks of nanodiffraction patterns do not provide a reliable estimate of the strain because the 2θ angle at which these reflections are observed depends on the random local orientations of individual mosaic blocks. The possibility that the shift to higher 2θ angles is due to a systematic change in the orientation of the mosaic blocks as a result of the domain writing process can be eliminated, however, by examining the photon energy dependence of the diffraction patterns, as described in the Supporting Information. A simulation gives excellent agreement with the observed diffraction patterns (dashed line, Figure 3c), with the assumption that the diffraction patterns consist of sharp reflections from coherent diffractions of two large mosaic blocks and a broad reflection from a large number of smaller blocks.

The difference in lattice spacing between written and unwritten domains can be more easily measured using the shift in the high-2θ edge of the diffraction patterns. Doing this allows us to extend the analysis of the diffraction pattern to a more general case in which we are not restricted to analyze regions with identical mosaic block structures. The compressive strain reaches 0.1% in the center of written domains with respect to the unwritten areas. The spatial variation of the strain is shown in Figure 4a, matching the phase of the PFM response acquired in the same locations (Figure 4b).

The compressive strain in written domains can be explained by noting that the surface charge of the written domains may not be completely compensated and that a depolarization field in the opposite direction of polarization can be developed within the written domains.[16] Air, dielectrics, and even conductors cannot completely compensate the polarization charge.[17,18] The written domains are compressively strained due to the electromechanical response to this charge. The electric field accompanying the strain induced by writing can be determined via the piezoelectric coupling. With a piezoelectric coefficient of 45 pm/V,[19] the observed 0.1% strain corresponds to a depolarization field of 220 kV/cm. This electric field is smaller than the low-frequency coercive field and is thus not sufficient by itself to completely destabilize the P_+ domain.

The compressive strain developed during ferroelectric nanolithography raises the free energy of the written domains and can lead to the destabilization of small ferroelectric nanodomains. The combination of this strain and the built-in field raise the free energy of the written domains, making the written state metastable. Only the relative difficulty of nucleating and growing domains of the lower-energy P_- polarization prevents a lowering of the free energy by the production of a single domain state. The large 1 μm domains written for these experiments thus persist over long intervals of weeks or more and appear in PFM images acquired after the X-ray studies. Smaller domains, however, can be expected to be considerably less stable. The dynamics of the decay of macroscopic polarization in the analogous two-dimensional thin film geometry has been studied extensively.[20,21] The formation and decay of domains written nanolithographically by PFM involve an inherently more complicated distribution of

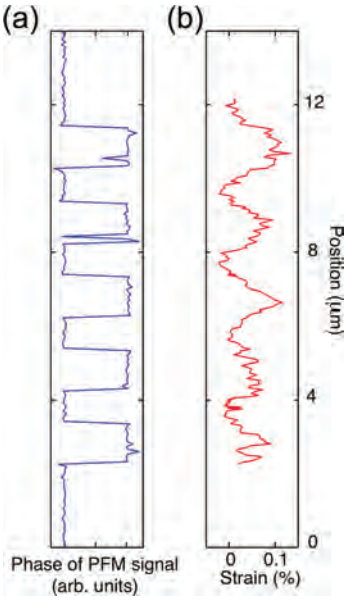

Figure 4. (a) Piezoelectric phase observed using PFM. (b) Compressive strain along a vertical line within the dashed rectangle in Figure 2a.

fields but follow similar considerations.[22] The decay of the written polarization state will be sped by the additional elastic energy we have found here.

X-ray nanodiffraction measurements show that local nanoscale structural effects can have a profound impact in scanning probe nanolithography and on future prospects for understanding and control of nanoscale phenomena. The evaluation of the distortions resulting from nanolithography leads to the future opportunity to develop nanotechnologies that allow the use of nanoscale variations in strain to select the ground state of ferroelectrics, dielectrics, and other complex oxides.[23−25] In addition, extensions of this approach will allow a detailed exploration of the connections between growth conditions, the selection of the direction of the ferroelectric polarization via these conditions, and the role of defects in the stability of domains. The match in length scales between the spatial resolution of X-ray nanoprobes and scanning probe lithography promises to reveal structural effects in emerging nanomaterial systems in which subtle degrees of freedom can be patterned at small scales including orbital and charge order[26] as well as ferromagnetic, ferrimagnetic, and antiferromagnetic moments.[27]

■ ASSOCIATED CONTENT

Supporting Information. Coherent diffraction simulation and distinguishing between strain and crystallographic rotation using the photon-energy-dependence of the diffraction pattern. This material is available free of charge via the Internet at http://pubs.acs.org.

■ AUTHOR INFORMATION

Corresponding Author

*E-mail: evans@engr.wisc.edu.

Present Addresses

[⊥]School of Materials Science and Engineering, Gwangju Institute of Science and Technology, Gwangju 500-712, Korea.

dx.doi.org/10.1021/nl2009873 |*Nano Lett.* XXXX, XXX, 000–000

■ ACKNOWLEDGMENT

P.E. acknowledges support by the U.S. Department of Energy through Contract No. DE-FG02-04ER46147 for the nanoprobe experiment and by the U.S. National Science Foundation through Grant No. DMR-0705370 for the photon-energy-dependent scattering study. C.B.E. acknowledges support by the National Science Foundation under Grant No. ECCS-0708759 and the Army Research Office under Grant No. W911NF-10-1-0362. Use of the National Synchrotron Light Source, Brookhaven National Laboratory, was supported by the U.S. Department of Energy, Office of Science, Office of Basic Energy Sciences, under Contract No. DE-AC02-98CH10886. Use of the Center for Nanoscale Materials was supported by the U.S. Department of Energy, Office of Science, Office of Basic Energy Sciences, under Contract No. DE-AC02-06CH11357.

■ REFERENCES

(1) Garcia, R.; Calleja, M.; Rohrer, H. *J. Appl. Phys.* **1999**, *86*, 1898–1903.
(2) Fenwick, O.; Bozec, L.; Credgington, D.; Hammiche, A.; Lazzerini, G. M.; Silberberg, Y. R.; Cacialli, F. *Nat. Nanotechnol.* **2009**, *4*, 664–668.
(3) Zou, S.; Maspoch, D.; Wang, Y.; Mirkin, C. A.; Schatz, G. C. *Nano Lett.* **2007**, *7*, 276–280.
(4) Gruverman, A; Tokumoto, H.; Prakash, A. S.; Aggarwarl, S.; Yang, B.; Wuttig, M.; Ramesh, R.; Venkatesan, T. *Appl. Phys. Lett.* **1997**, *71*, 3492–3494.
(5) Krause, S.; Berbil-Bautista, L.; Herzog, G.; Bode, M.; Wiesendanger, R. *Science* **2007**, *317*, 1537–1540.
(6) Zhang, J. X.; Xiang, B.; He, Q.; Seidel, J.; Zeches, R. J.; Yu, P.; Yang, S. Y.; Wang, C. H.; Chu, Y.-H.; Martin, L. W.; Minor, A. M.; Ramesh, R. *Nat. Nanotechnol.* **2011**, *6*, 98–102.
(7) Kalinin, S. V.; Jesse, S.; Rodriguez, B. J.; Eliseev, E. P.; Gopalan, V.; Morozovska, A. N. *Appl. Phys. Lett.* **2007**, *90*, 212903.
(8) Shu, D.; Maser, J.; Holt, M; Winarski, R. P.; Preissner, C.; Smolyanitskiy, A.; Lai, B.; Vogt, S.; Stephenson, G. B. Ninth International Conference on Synchrotron Radiation Instrumentation. *AIP Conf. Proc.* **2007**, *879*, 1321–1324.
(9) Pintilie, L.; Stancu, V.; Trupina, L.; Pintilie, I. *Phys. Rev. B* **2010**, *82*, 085319.
(10) Baek, S. H.; Jang, H. W.; Folkman, C. M.; Li, Y. L.; Winchester, B.; Zhang, J. X.; He, Q.; Chu, Y. H.; Nelson, C. T.; Rzchowski, M. S.; Pan, X. Q.; Ramesh, R.; Chen, L. Q.; Eom, C. B. *Nat. Mater.* **2010**, *9*, 309–314.
(11) Ying, A.; Osting, B.; Noyan, I. C.; Murray, C. E.; Holt, M.; Maser, J. *J. Appl. Crystallogr.* **2010**, *43*, 587–595.
(12) Do, D.-H.; Evans, P. G.; Isaacs, E. D.; Kim, D. M.; Eom, C. B.; Dufresne, E. M. *Nat. Mater.* **2004**, *3*, 365–369.
(13) Als-Nielsen, J.; McMorrow, D. *Elements of modern X-ray physics*; John Wiley & Sons Ltd.: New York, 2001.
(14) Noheda, B.; Gonzalo, J. A.; Cross, L. E.; Guo, R.; Park, S.-E.; Cox, D. E.; Shirane, G. *Phys. Rev. B* **2000**, *61*, 8687–8695.
(15) XOP 2.3, available at http://www.esrf.eu/UsersAndScience/Experiments/TBS/SciSoft/xop2.3.
(16) Kalinin, S. V.; Bonnell, D. A. *Phys. Rev. B* **2001**, *63*, 125411.
(17) Fong, D. D.; Kolpak, A. M.; Eastman, J. A.; Streiffer, S. K.; Fuoss, P. H.; Stephenson, G. B.; Thompson, C.; Kim, D. M.; Choi, K. J.; Eom, C. B.; Grinberg, I.; Rappe, A. M. *Phys. Rev. Lett.* **2006**, *96*, 127601.
(18) Junquera, J.; Ghosez, P. *Nature* **2003**, *422*, 506–509.
(19) Grigoriev, A.; Sichel, R.; Lee, H. N.; Landahl, E. C.; Adams, B.; Dufresne, E. M.; Evans, P. G. *Phys. Rev. Lett.* **2008**, *100*, 027604.
(20) Bratkovsky, A. M.; Levanyuk, A. P. *Phys. Rev. Lett.* **2008**, *100*, 149701.
(21) Grigoriev, A.; Sichel, R. J.; Jo, J. Y.; Choudhury, S.; Chen, L.-Q.; Lee, H. N.; Landahl, E. C.; Adams, B. W.; Dufresne, E. M.; Evans, P. G. *Phys. Rev. B* **2009**, *80*, 014110.
(22) Morozovska, A. N.; Eliseev, E. A.; Svechnikov, S. V.; Krutov, A. D.; Shur, V. Y.; Borisevich, A. Y.; Maksymovych, P.; Kalinin, S. V. *Phys. Rev. B* **2010**, *81*, 205308.
(23) Pertsev, N. A.; Zembilgotov, A. G.; Tagantsev, A. K. *Phys. Rev. Lett.* **1998**, *80*, 1988–1991.
(24) Haeni, J. H.; Irvin, P.; Chang, W.; Uecker, R.; Reiche, P.; Li, Y. L.; Choudhury, S.; Tian, W.; Hawley, M. E.; Craigo, B.; Tagantsev, A. K.; Pan, X. Q.; Streiffer, S. K.; Chen, L. Q.; Kirchoefer, S. W.; Levy, J.; Schlom, D. G. *Nature* **2004**, *430*, 758–761.
(25) Cao, J.; Ertekin, E.; Srinivasan, V.; Fan, W.; Huang, S.; Zheng, H.; Yim, J. W. L.; Khanal, D. R.; Ogletree, D. F.; Grossman, J. C.; Wu, J. *Nat. Nanotechnol.* **2009**, *4*, 732–737.
(26) Renner, Ch.; Aeppli, G.; Kim, B.-G.; Soh, Y.-A.; Cheong, S.-W *Nature* **2002**, *416*, 518–521.
(27) Wolf, S. A.; Awschalom, D. D.; Buhrman, R. A.; Daughton, J. M.; von Molnár, J. M.; Roukes, M. L.; Chtchelkanova, A. Y.; Treger, D. M. *Science* **2001**, *294*, 1488–1495.

dx.doi.org/10.1021/nl2009873 |*Nano Lett.* XXXX, XXX, 000–000